Detection of Lead in Soil with Excimer Laser Fragmentation Fluorescence Spectroscopy

J. H. CHOI, C. J. DAMM, N. J. O'DONOVAN, R. F. SAWYER, C. P. KOSHLAND, and D. LUCAS*

Mechanical Engineering Department, University of California, Berkeley, California 94720 (J.H.C, N.J.O., R.F.S.); Science & Technology Department, Sierra Nevada College, Nevada 89451 (C.J.D.); School of Public Health, University of California, Berkeley, California 94720 (C.P.K.); and Environmental Energy Technologies Division, Lawrence Berkeley National Laboratory, Berkeley, California 94720 (D.L.)

Index Headings: **Photofragmentation; Fluorescence; Photochemistry; Plasma; Lead.**

INTRODUCTION

Lead (Pb) poisoning from environmental and occupational exposure remains one of the most common and preventable diseases. There are numerous serious and detrimental health effects from inhalation or ingestion of lead, including poisoning or even death in extreme circumstances.[1] Of particular concern are central nervous system impacts, particularly sub-clinical and clinical developmental effects in young children who are more likely to have contact with soils and dusts containing lead.[2,3] Sensitive rapid analytic techniques are needed for exposure assessment and remediation verification. Conventional wet-chemistry techniques require laborious and time-consuming processes, such as preparation, dissolution, chelation, and ion exchange.[4] Various *in situ*, real-time methods to measure heavy metals in soil have been developed; chemical analysis of a soil sample with spectroscopic methods is often achieved with much less sample preparation and time, but there are often difficulties with calibration, matrix effects, and sensitivity.[5,6]

Here we apply excimer laser fragmentation fluorescence spectroscopy (ELFFS) to pure lead nitrate salts and soils doped with lead nitrate. We and other groups have used ELFFS to monitor various gaseous hydrocarbons, ammonia, combustion generated metal species, and soot particles from diesel and other combustion exhausts.[7–11] The main difference between this method and other direct solid ablation analysis techniques, such as laser-induced breakdown spectroscopy (LIBS) or laser ablation, is that the surface is photolyzed at laser fluences below the threshold where plasma formation occurs. The method benefits from an increased signal-to-noise (S/N) ratio compared with LIBS since the lack of a plasma eliminates the strong continuum emission that interferes with the analyte signals. The emission from the sample surface is recorded during the laser pulse without gating, and the emission peak is normally proportional to the concentration of the emitting species.[12]

EXPERIMENTAL

A schematic of the experimental apparatus is shown in Fig. 1. Photons of 193 nm and with a pulse duration of 20 ns are emitted from an ArF excimer laser (Lambda Physik LPX 210i). The laser beam is focused with a 3.8 cm diameter, 25 cm focal length UV grade fused silica lens, and a 5 cm diameter mirror redirects the beam onto the solid surface of the sample. Laser fluences range from 0.4 to 4 J/cm^2. The fluence is varied by changing the voltage of the laser and/or by introducing screens in the beam path. Fluorescence is collected with a 3.8 cm biconvex lens (f# of 1.0) onto the entrance slit of a 0.3 m CGA/McPherson scanning monochromator. The slit width of the monochromator is 0.4 mm, corresponding to a 1.1 nm bandpass. The light from the monochromator is detected by a Pacific 508 photomultiplier tube, and the signal is digitized by a LeCroy LT 342 digital oscilloscope and transferred to a PC through a GPIB cable for further analysis.

Two different sample plates are used: the first plate is a flat anodized aluminum plate; the second has two wells machined 2 mm into the surface to hold the solid samples. The wells allow us to reproducibly fill the sample to the same level and contain the solids when ablating at high laser fluences. The sample plate is on a mounting system in the laser interrogation region that includes a magnetic connection and vertical translational stage to insure repeatability of a desired position and the optimal height of the test plate, respectively. The sample plate can also be horizontally translated with a motor or manually to introduce a fresh sample into the laser interrogation region. The aluminum plate was found to have a low scattering background, with no atomic or ionic Al peaks evident at the energy levels used here. Lead nitrate ($Pb(NO_3)_2$), (Aldrich, 99+%) is used pure and in a mixture with soil. Pure lead nitrate is dissolved in water and applied to one of the sample wells. The solution is dried with a heat lamp or gun. Soil was obtained from a residential garden in Berkeley, California. It was ground using a mortar and pestle and sifted using a coarse screen

Received 5 February 2004; accepted 20 October 2004.

* Author to whom correspondence should be sent. E-mail: d_lucas@lbl.gov.

0003-7028/05/5902-0258$2.00/0

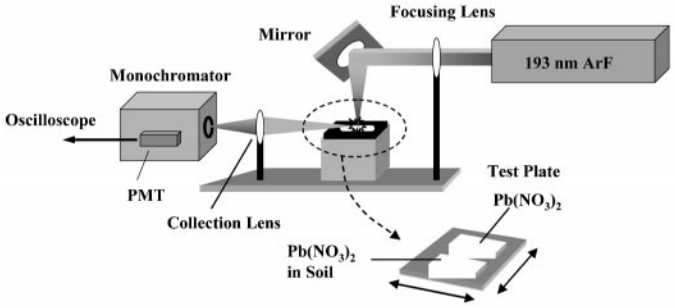

FIG. 1. Schematic of the experimental apparatus.

(1.5×1.5 mm^2). A measured amount of a known concentration lead nitrate solution is added to the soil to obtain a slurry. The slurry is applied to the other sample well, and then dried.

RESULTS AND DISCUSSION

The emission spectrum from $Pb(NO_3)_2$ and the background signal are shown in Fig. 2. The peak value of the emission during a time window of approximately 100 ns around the laser pulse is recorded for each single shot. The spectrum presented was collected at a laser fluence of 0.4 J/cm^2. The monochromator was scanned at a rate corresponding to 5 shots/nm, and a rolling average of 5 shots was used to smooth the data. The background signal is obtained directly from the anodized surface and contains both optical and electrical noise. In the background spectrum the only peak observed is the second order of the laser scattering at 386 nm. The lead emission spectrum also shows five distinctive emission lines of lead atoms at 357.2, 364.0, 368.3, 373.9, and 405.8 nm. The 405.8 nm peak, a commonly used emission line for Pb analysis owing to its strong emission, involves electronic transitions from $7s^1\,^3P$ to $6p^2\,^3P$. Note that at this fluence there is little broadband emission associated with plasma formation.

The time-resolved emission from $Pb(NO_3)_2$ at 405.8 nm and the background signal at 415 nm are presented in Fig. 3. The signals are shifted in time to a common scale, as the different laser conditions affect the time at which lasing actually occurs. The decay times for these signals are shown in Table I.

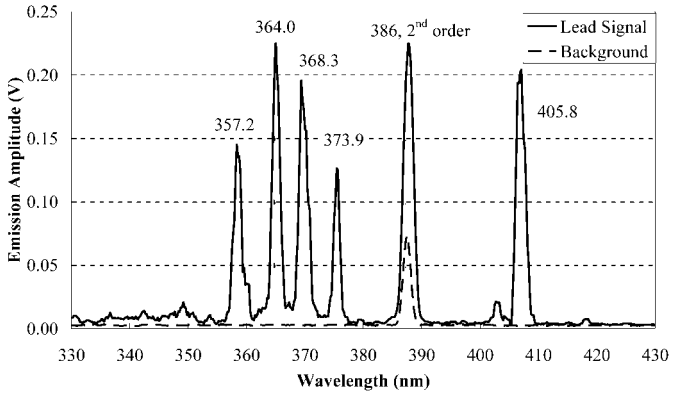

FIG. 2. Emission spectra of background from the anodized Al surface and lead from $Pb(NO_3)_2$ at the laser fluence of 0.4 J/cm^2.

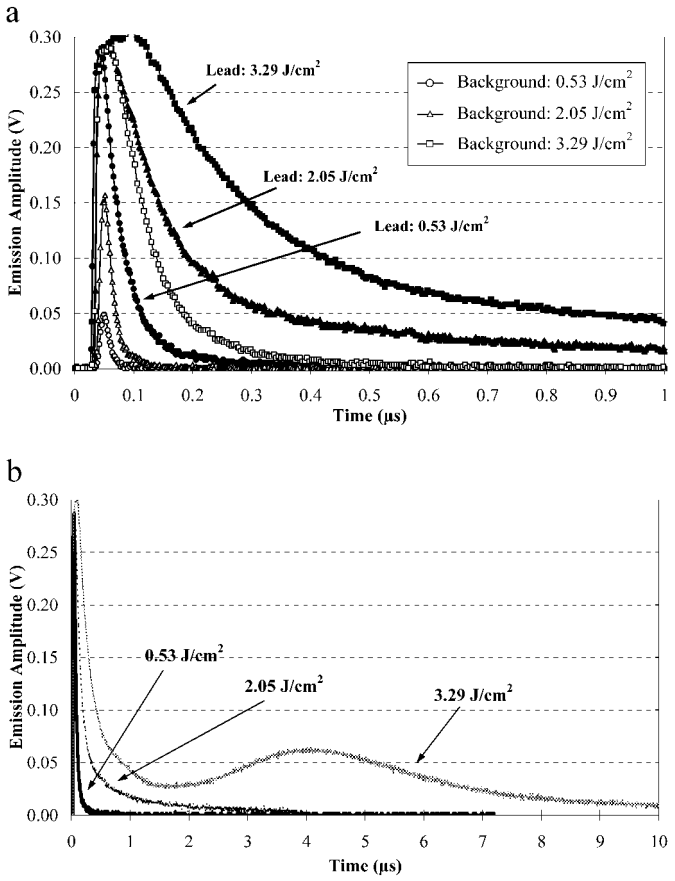

FIG. 3. Time-resolved emission from $Pb(NO_3)_2$ (405.8 nm) and background (415 nm) at various fluence conditions. (**a**) Emission during the first microsecond. (**b**) Lead emission at longer time scales. Note that plasma formation threshold appears at approximately 2 J/cm^2.

There are several points to consider in these results. During the first microsecond (Fig. 3a) at the lowest fluence, 0.53 J/cm^2, the background signal is relatively low (0.05 V) and lasts about as long as the laser pulse. Similar signals are observed at other wavelengths not associated with known transitions, and when we use different wavelengths for the background signal the results are not significantly different. The background is mainly due to 193 nm laser light leaking through the monochromator (its rejection ratio is approximately 4000:1). The signal from lead at these conditions peaks near 0.3 V and lasts longer. At higher fluences, the peak of the lead emission does not increase, but the emission tail grows. The background signal increases dramatically, reaching the same peak value as the lead emission at the highest fluence (3.29 J/cm^2). We, as well as others, have previously observed that the peak signal is not a strong function of laser fluence, presumably since the process has a step that can be saturated.[11,13]

TABLE I. Characteristic exponential decay time of the signals produced by photofragmentation fluorescence (* denotes the decay time of the first peak).

Fluence	0.53 J/cm^2	2.05 J/cm^2	3.29 J/cm^2
Lead	41 ns	126 ns	284 ns*
Background	12 ns	16 ns	74 ns

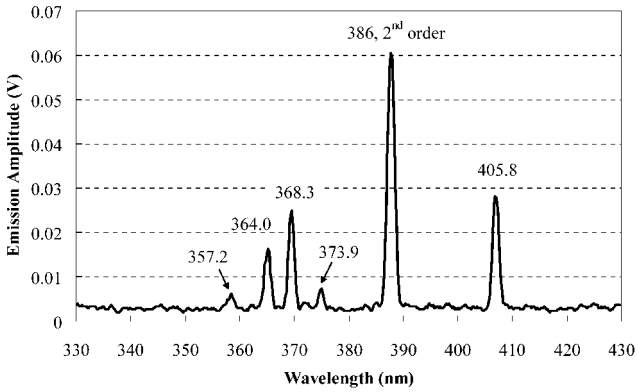

FIG. 4. Emission spectrum of Pb in soil for the laser energy of 30 mJ. Note that five lead emission peaks can be clearly recognized. The Pb concentration is estimated to be several thousand ppm.

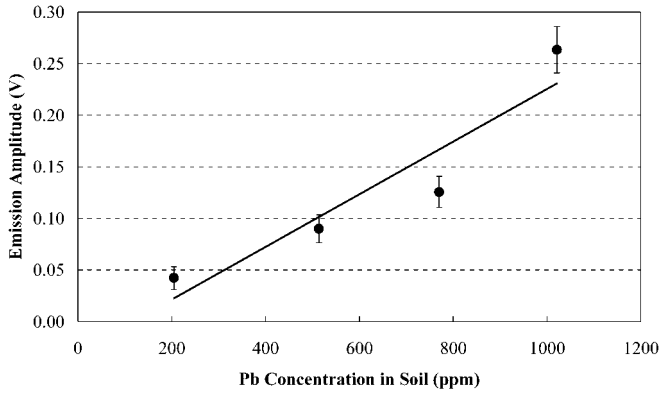

FIG. 5. Correlation curve for lead emission and concentration of lead added to the soil. The presented values are the difference between the maximum lead emission at 405.8 nm and the background measured at 345 nm for two different laser shots. 345 nm was chosen because there is no emission expected from known species. The laser energy is 260 mJ.

Even more dramatic changes are observed at longer times (Fig. 3b). At fluences below 2 J/cm^2 the signal is a single peak with a near exponential decay. At higher fluences, a second peak emerges at longer times, peaking in the 3–5 μs range. At the lower fluences, atoms or molecules are released from the matrix through direct photochemical bond breaking rather than through photothermal processes, since the 193 nm photons are energetic enough to break most of the molecular bonds. As the fluence increases, more species are liberated and electronically excited and a higher fraction of species is ionized. Above the threshold, the extent of fragmentation and ionization increases, and the liberated and ionized species absorb the incoming light, forming a plasma. Plasma formation has been widely studied using laser ablation or laser breakdown techniques.[14–16]

Once a plasma plume is formed by accumulation of photon energy at high fluence, incoming light is absorbed and emission is trapped within a plasma so that the plume grows, reaching an elevated temperature (5000~15 000 K) and triggering broadband emission from air, electrons, atomic or ionic species, and ablated fragments. After the plume of the fully grown plasma cools, the analyte emission forms another peak as shown in Fig. 3b, which is characteristic of Pb emission in LIBS. The lifetime of the signal in this case extends to 10 μs. Note that the magnitude of the background peak linearly increases with the fluence and reaches the same as that from $Pb(NO_3)_2$ while lead signal intensities are almost unchanged. Therefore, it can be expected that if the background is subtracted from the lead emission, the net signal will decrease with increasing fluence. By using lower fluences and avoiding plasma formation, we significantly achieve better signal-to-noise ratios. The temperature increase in the gas phase and changes in collisional quenching are not significant compared to cases with a plasma. Finally, photon energy transfer to the target material is more efficient and there is no need for signal gating and time-resolved data analysis.

The same measurement procedure is applied to soil samples with lead nitrate salt added, where the sample surface is significantly rougher. The spectrum of lead added to the soil is shown in Fig. 4. The spectrum of pure soil does not contain any obvious distinct peaks except ones from laser scattering (not shown here). However, the noise level from background soil is often considerably higher than that from anodized Al plate, so the laser energy is reduced to optimize S/N, and the five emission lines of lead are still observed. As with the pure lead nitrate, the lead signal increases with laser fluence, but the background increases at a faster rate.

Direct application of spectroscopic techniques for metal detection in soils without any sample preparation has limits since soil is inherently inhomogeneous in nature. It is not expected that the target species is contained uniformly in soil, so variations could easily occur in different locations from a sample. The surface roughness and material properties of the soil is also not uniform. When focused on a single point, the laser eventually craters the soil surface, which affects both the laser–soil interaction and the detection sensitivity. We minimized the crater effect by introducing a fresh sample into the probe volume approximately at the translational rate of 0.11 mm/s. In addition, Eppler et al.,[17] Wisbrun et al.,[18] Bulatov et al.,[6] and Capitelli et al.[5] showed that various types of soil interact differently with photons during laser-induced plasma formation, and in turn, the recorded signals have different characteristics.

Figure 5 shows the relationship between the peak emission amplitude with the lead concentrations in soil. The values shown are the difference in maximum lead emission and background at 405.8 and 345 nm, respectively. The resulting signal is roughly linear with concentration, and indicates that the method could be used to quickly screen samples without significant preparation. The detection limit for our system, defined as the point where the peak emission signal is three times the standard deviation of the background, is approximately 200 ppm. The detection limit is lower than the regulatory standards imposed by US EPA for the presence of lead in soil (400 ppm[19]). The sensitivity of the system is dominated by optics and sample conditions, such as alignment, laser fluence, sample preparation, and the soil matrix. While additional work is

needed to ascertain the robustness of the analytical method, the lack of spectral interference from plasma-type emission is certainly promising.

CONCLUSION

Excimer laser fragmentation fluorescence spectroscopy using a 193 nm ArF excimer laser was used to detect atomic Pb emission from solid $PbNO_3$ and $PbNO_3$ mixed into a soil. The detection method differs from other solid ablation processes in that lower laser fluences can be used where there is no plasma generation and subsequent broadband emission; fluences above 2 J/cm^2 resulted in plasma formation. The detection limit for $PbNO_3$ in a single soil type is about 200 ppm, achieved with minimal sample preparation and an analysis time on the order of a minute. The technique holds promise as a rapid and sensitive method for processing soil samples for assessing exposures or the effectiveness of soil remediation.

ACKNOWLEDGMENT

This work was supported by the Environmental Health Sciences Superfund Basic Research Program (Grant Number P42ESO47050-01) from the National Institute of Environmental Health Sciences, NIH, with funding provided by the EPA. The authors thank the Wood-Calvert Chair in Engineering for additional support. The contents of the work are solely the responsibility of the authors and do not necessarily represent the official views of NIEHS, NIH, or EPA.

1. USEPA, 747-R-97-006 (1998).
2. H. L. Needleman, C. Gunnoe, A. Leviton, R. Reed, H. Peresie, C. Maher, and P. Barrett, N. Engl. J. Med. **300,** 689 (1979).
3. G. A. Wasserman, X. Liu, N. J. Lolocono, P. Factor-Litvak, J. K. Kline, D. Popovac, N. Morina, A. Musabergovoc, N. Vrenezi, S. Capuni-Paracka, V. Lekic, E. Preteni-Redjepi, S. Hadzialjevic, V. Salkovich, and J. H. Graziano, Environ. Health Perspect. **105,** 956 (1997).
4. F. Hilbk-Kortenbruck, N. Reinhard, P. Wintjens, F. Heinz, and C. Becker, Spectrochim. Acta, Part B **56,** 933 (2001).
5. F. Capitelli, F. Colao, M. R. Provenzano, R. Fantoni, G. Brunetti, and N. Senesi, Geoderma **106,** 45 (2002).
6. V. Bulatov, R. Krasniker, and I. Schechter, Anal. Chem. **70,** 5302 (1998).
7. C. J. Damm, D. Lucas, R. F. Sawyer, and C. P. Koshland, Chemosphere **42,** 655 (2001).
8. S. G. Buckely, D. Lucas, C. P. Koshland, and R. F. Sawyer, Combust. Sci. Technol. **118,** 169 (1996).
9. C. S. McEnally, D. Lucas, C. P. Koshland, and R. F. Sawyer, Appl. Opt. **33,** 3977 (1994).
10. B. L. Chadwick, G. Domazetis, and R. J. S. Morrison, Anal. Chem. **67,** 710 (1995).
11. R. C. Sausa, A. J. Alfano, and A. W. Miziolek, Appl. Opt. **26,** 3588 (1987).
12. N. J. O'Donovan, M.S. Thesis, Mechanical Engineering Department, University of California at Berkeley, Berkeley, California (2002).
13. S. G. Buckley, C. J. Damm, W. M. Vitovec, L. A. Sgro, R. F. Sawyer, C. P. Koshland, and D. Lucas, Appl. Opt. **37,** 8382 (1998).
14. W. F. Ho, C. W. Ng, and N. H. Cheung, Appl. Spectrosc. **51,** 87 (1997).
15. D. S. Tomson and D. M. Murphy, Appl. Opt. **32,** 6818 (1993).
16. J. E. Carranza and D. W. Hahn, Anal. Chem. **74,** 5450 (2002).
17. A. Eppler, D. A. Cremers, D. D. Hickmott, M. J. Ferris, and A. C. Koskelo, Appl. Spectrosc **60,** 1175 (1996).
18. R. Wisbrun, I. Schechter, R. Niessner, H. Schroder, and K. L. Kompa, Anal. Chem. **66,** 2964 (1994).
19. USEPA, 40 CFR Part 745 (2001).

An Internal Standardization Procedure for Spectrally Resolved Fluorescence Lifetime Imaging

QUENTIN S. HANLEY* and V. RAMKUMAR†

Department of Biological and Chemical Sciences, University of the West Indies, Cave Hill Campus, St. Michael, Barbados

Index Headings: **Fluorescence lifetime imaging; FLIM; Spectrally resolved FLIM; Frequency domain; Standardization; Fluorescence.**

INTRODUCTION

Fluorescence lifetime imaging (FLIM) is typically done in a two-dimensional imaging mode without measuring the entire lifetime spectrum. The introduction of an imaging spectrograph into the detection path of the lifetime instrument allows the lifetime spectrum to be observed, including the lifetime signature of any excitation light passing through the emission filter of the microscope. Excitation light leaking into the detection path of a conventional FLIM system is detrimental to the measurement of the lifetimes, since it causes a variable mixing of a short lifetime component into the data. However, by intentionally allowing excitation laser light to enter a spectrally resolved FLIM (sFLIM) detection system, an internal standardization may be provided by comparing the modulation depth and phase shift of the laser light to that of a standard. Such an approach stabilizes the lifetime measurement obtained from a system over time and can reduce the time between measurements by eliminating external standardization. Long-term stabilization is particularly important in drug screening instruments requiring a combination of high-speed and high-stability measurements. Internal standardization can be implemented in sFLIM using a scattering surface and a holographic notch filter. Although this light does not travel the same optical path though the microscope as the fluorescence excitation and emission light, the path length difference can be calibrated, and following calibration it may be used to increase the speed and stability of spectrally resolved FLIM measurements. When compared directly to an external standardization procedure improved accuracy and precision were observed while potentially improving the throughput of sFLIM instrumentation.

Fluorescence lifetime imaging in either the time[1–3] or frequency[4–6] domain is becoming a mature method for investigating proximity relationships in intact cellular systems.[7,8] A variety of commercial instruments are available as additions to wide field and confocal microscopes and approaches have been described for the analysis of mixtures[9] and functional imaging.[7,10,11] In the time do-

Received 3 August 2004; accepted 11 October 2004.

* Author to whom correspondence should be sent. E-mail: qhanley@uwichill.edu.bb.

† Current address: Department of Chemistry, Indian Institute of Technology Madras, Chennai, India.